[Dye Molecules/Copper(II)/Macroporous Glutaraldehyde-Chitosan] Microspheres Complex: Surface Characterization, Kinetic, and Thermodynamic Investigations

Mahjoub Jabli,[1] M. H. V. Baouab,[2] N. Sintes-Zydowicz,[3] Bechir Ben Hassine[1]

[1]*Laboratoire de Synthèse Organique Asymétrique et Catalyse Homogène, Department de chimie, Faculté des Sciences de Monastir, Avenue de l'Environnement 5019 Monastir, Tunisie*
[2]*Institut Préparatoire aux Etudes d'Ingénieurs de Monastir, Rue Ibn El Jazzar 5019 Monastir, Tunisie*
[3]*Laboratoire des Matériaux Polymères et des Biomatériaux, Department de chimie, Bât. ISTIL, Université Claude Bernard LYON 1, UMR CNRS 5627 15, Boulevard Latarjet, 69622, Villeurbanne, France*

Received 29 September 2010; accepted 11 March 2011
DOI 10.1002/app.34519
Published online 15 September 2011 in Wiley Online Library (wileyonlinelibrary.com).

ABSTRACT: Chitosan microspheres loaded Cu(II) were prepared using a precipitation method and heterogeneously crosslinked with glutaraldehyde. The abilities of the binary [Cu(II)/Glut-chitosan] system for binding two acid dyes, that is, Acid blue 25 (AB25) and Calmagite (Calma) were investigated. Sorption experiments were performed using a batch process at 25°C and indicate pH dependence. Evidence for the modification of the raw chitosan polymer was provided by Fourier transform infra red spectral study, thermogravimetry, differential thermogravimetry, differential scanning calorimetry, and scanning electron microscopy analysis. Data gleaned from the thermal analyses, showed that the modification of the polymer decreases the thermal stability of the prepared materials with respect to that of the native one. The effecting factors during dye adsorption have been also studied. Thermodynamic and kinetic experiments were undertaken to assess the capacity and the rate of dyes removal on the surface of [Cu(II)/Glut-chitosan]. Experimental data were mathematically described using various kinetic models. The pseudo second-order equation was shown to fit the adsorption kinetics. The interpretation of the equilibrium sorption data complies well with the Freundlich adsorption model. Thermodynamic results indicate that the adsorption follows an exothermic process. © 2011 Wiley Periodicals, Inc. J Appl Polym Sci 123: 3412–3424, 2012

Key words: chitosan microspheres; glutaraldehyde; Cu(II); AB25; calma; sorption; thermal analysis; thermodynamic; kinetic models

INTRODUCTION

The chemical contamination of water with toxic derivatives is a serious environmental problem. Attention has been focused on the use of several technologies to treat such resources.[1–3] Compared with the expensive physical or chemical procedures, adsorption process provides an alternative and receives increasing interest. More importantly, studies have been carried out to develop more effective and selective adsorbent materials, which are abundant in nature and require little processing. Among these low cost adsorbents, activated carbon,[4] silica,[5] cellulose,[6,7] and, more recently, chitin and chitosan[8–10] are the most extensively investigated. In this framework, numerous studies have demonstrated the effectiveness of chitosan and its derivatives products to remove metals, such as: arsenic,[11] cadmium,[12–14] copper,[12,15–21] lead,[13] mercury,[22–24] molybdenum,[23,25] nickel,[12,16] vanadium,[23] uranium,[24] zinc,[12,13] etc. In other areas, chitosan has been employed as an excellent adsorbent for the sorption of dyes,[26,27] phenols,[28] enzymes,[29] protein separations,[30] and in some enzyme immobilizations procedures.

However, compilation of the literature does not indicate any use of the chitosan microspheres, particularly, in the field of both metal and acid dye sorption systems and no ternary complex has been prepared and characterized. For example, Sulakova et al., [31] have only investigated on the use of Cu(II) chitosan complexes as heterogeneous catalysts for the degradation of five model azo textile dyes in aqueous solution using hydrogen peroxide as an oxidant. Shen et al., [32] have described the oxidation of Acid red 73 using chitosan microspheres supported Cobalt (II) tetrasulfophthalocyanine. Vasconcelos and coworkers, [17] involved the preparation of chitosan microspheres containing a reactive dye Orange as a chelating agent by spray drying technique. The obtained new adsorbent was used in batch experiments to evaluate the

Correspondence to: B. B. Hassine (bechirbenhassine@yahoo.fr).

Contract grant sponsors: DGRSRT (Direction Générale de la Recherche Scientifique et de la Rénovation Technologique) of the Tunisian Ministry of Higher Education, Scientific Research and Technology, Tunis, Tunisie.

adsorption of Cu(II) and Cd(II) ions in single and binary metal solutions.[17]

Chelating polymeric adsorbents have found widespread applications in the field of the removal of hazardous and environmentally undesirable chemicals from waste streams. Cellulose derivatives have been particularly investigated during the treatment of effluents.[33–35] In a previous work, Baouab et al., [7] have chemically modified the cotton fiber by ethylene diamine and then the ethylene diamine-grafted groups immobilizes Cu(II) ions was tested for the adsorption of Calma and AB25 as ligands in the metal-coordinating process.

The objectives of this article concern the description, for the first time, of the feasibility and the characterization of a ternary complex formation between the two model ligands (AB25 and Calma), Cu (II) ions, and crosslinked chitosan microspheres using a batch process under several experimental conditions. The effects of pH, initial concentration, agitation period, and temperature on the adsorption rate of Calma and AB25 on the surface of the binary system have been developed. The prepared materials were characterized using Fourier Transform Infra Red (FTIR), thermogravimetry (TG), differential scanning calorimetry (DSC), and scanning electron microscopy (SEM) analyses to allow verifying a structural difference between the started and the modified compounds. Hence, a probable reaction mechanism of the ternary complex formation was proposed. Thermodynamic and kinetic experiments were also evaluated. Experimental kinetic data were mathematically described using adsorption kinetic models, namely pseudo first-order, pseudo second-order, elovich equation, and intraparticle diffusion models. With regards to its main use (adsorption of the pollutants from aqueous solution), this complex could has the possibility of being valorized as an effective adsorbent in terms of Cu(II) ions sorption by a binary system [Cu(II)/Glut-chitosan] or dye and Cu(II) ions sorption by a ternary complex [Dye/Cu(II)/Glut-chitosan] microspheres.

EXPERIMENTAL

Materials and reagents

Chitosan from crab shell (deacetylation degree = 72.5) was purchased from Aldrich (ς-Aldrich Chimie Sarl, Saint-Quentin Fallavier, France) as a powder material. All other chemicals [glutaraldehyde (25% v/v aqueous solution), glacial acetic acid, and sodium hydroxide] were of analytical grade used without further purification. Stock solutions of Cu(II) were prepared by dissolving $CuCl_2.2H_2O$ in distilled water and whose initial pH were adjusted by NaOH or HCl (0.10 mol L^{-1}). The dyes used in the adsorption experiments, namely Acid Blue 25 and Calmagite [referred to as AB25 (molar weight = 416.39 g mol^{-1}) and Calma (molar weight = 358.37 g mol^{-1}), respectively], were supplied by Hoechst (Frankfort, Germany) in the form of sodium salt and known for their capacity of metal complexation due to the presence of donor atoms in their structures indicated in Figure 1. The presence of functional groups (hydroxyl) and electron donor atoms (oxygen and/or nitrogen) allows these ligands to build complexes with metal ions. These anionic dyes were also used without further purification.

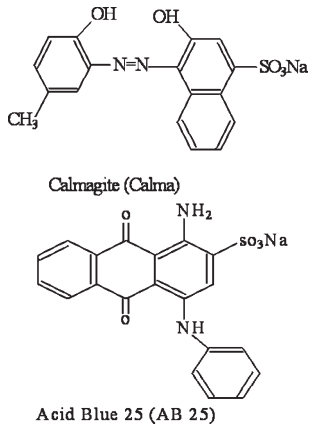

Figure 1 Chemical structure of the selected dyes.

Preparation of macroporous Glut-chitosan microspheres

Chitosan microspheres were synthesized by drop wise addition of an acidic chitosan solution into a sodium hydroxide solution precipitation bath. A 2% (w/v) chitosan solution was prepared by dissolving 2 g of powdered chitosan into 100 mL of 5% (v/v) glacial acetic acid solution at room temperature to produce a viscous solution. After complete mixing, it was forced through a micropipette tip by a ROTH® peristaltic pump. The solution was carried out through a nozzle (inner diameter = 0.20 mm) and dropped into a bath containing a 2.0 mol L^{-1} NaOH solution and chitosan microspheres were quickly formed. The reaction of acetic acid with the NaOH caused the precipitation of chitosan in solution resulting in gelled microspheres. Prepared microspheres were allowed to harden in this solution for 24 h. Subsequently, chitosan microspheres were filtered and rinsed several times with distilled water up to neutral pH.[36]

For crosslinking with Glutaraldehyde, Glut-chitosan microspheres were prepared according to the following procedure described previously.[37] Chitosan microspheres were heterogeneously crosslinked by immersion in 0.75% (w/w) aqueous 25% v/v

glutaraldehyde solution (3.0 g of wet chitosan microspheres in 50 mL of glutaraldehyde solution) at a temperature of 25°C for 2 h, followed by rinsing with deionized water to remove any unreacted glutaraldehyde and stored in water at 4°C. As the sorption conditions required the use of the chitosan microspheres in a wide range of pH, the crosslinking treatment aims to resolve the solubility of the plain polymer in acidic pH. This makes it useful for the removal of chemical pollutants in acidic solution.[38]

To allow a comparison between the present results and the experimental data from the literature, the water content measurement in Glut-chitosan microspheres can generally be reached using an established conversion factor. The conversion factor of wet-base to Glut-chitosan microspheres is given in eq. (1). This was measured by weighting the wet adsorbent, which was oven-dried (at 70°C) for 24 h and weighted again. The calculated percent hydration rate was found to be equal to 97.50% and was evaluated using the following equation:

$$\text{Hydration rate } (\%) = \frac{(W_{\text{wet}} - W_{\text{dry}})}{w_{\text{wet}}} \times 100 \quad (1)$$

W_{wet} and W_{dry} are the weight of the wet and dry Glut-chitosan microspheres, respectively. Measuring error for water content value was 10^{-3}%. It is interesting to observe that this value is comparable to the data found by Li and Bai (the hydration rate is close to 97.29%).[39]

Loading of Glut-chitosan microspheres with Cu(II) ions

To load Glut-chitosan microspheres with Cu(II) ions up to saturation, a desired amount of the solid support with an aqueous solution of Cu(II) ions were stirred for 24 h at room temperature in a closed vessel. The pH was adjusted to the desired value with 0.10*M* HCl and/or 0.10*M* NaOH. The wet Glut-chitosan microspheres loaded Cu(II) was filtered off, washed with distilled water, and stored in distilled water at 4°C until further use. The initially yellow color of Glut-chitosan microspheres becomes blue turquoise after adsorption of Cu(II) ions. Indeed, the amine groups present in chitosan chains are the main effective bonding sites for metallic ions, resulting in complexes stabilized by coordination.[21] The characterization of all prepared solid materials was then performed by FTIR spectroscopy, TG, differential thermogravimetry (DTG), DSC, and SEM analyses.

Characterization of prepared supports

The FTIR characterization of the raw chitosan polymer, Glut-chitosan microspheres, the binary [Cu(II)/Glut-chitosan] system, and the ternary [dye/Cu(II)/Glut-chitosan] complex was carried using a FTIR spectrometer (Perkin–Elmer FTIR System 2000 Model spectrometer, LMPB, ISTIL Lyon 1 Villeurbanne, France). Samples were dispersed in anhydrous spectrophotometric potassium bromide (KBr) in 1 : 10 ratio. The range from 4000 to 400 cm^{-1} was scanned. Prepared supports were also characterized using thermogravimetric analysis (TGA 2950 instrument, LMPB, ISTIL Lyon 1 Villeurbanne, France) and Differential Scanning Calorimetry (DSC 2920 TA Instruments, LMPB, ISTIL Lyon 1 Villeurbanne, France). The measurements were performed, with a heating rate of 10°C min^{-1}, in a dynamic N_2 atmosphere on $\sim$ 5–10 mg of the sample. The scanning temperature range was from 25 to 900°C for TGA and from 25 to 350°C for DSC. The morphology and the surface structure of the prepared solid supports were evaluated using SEM analyses (Hitachi S800-1 Scanning Electron Microscopy, LMPB, ISTIL LYON 1 France). The concentration of the Cu(II) ions, AB25, and Calma was analyzed by an ultraviolet-visible spectrophotometer (U-2000 Hitachi, LMPB, ISTIL Lyon 1 Villeurbanne, France) with 2 nm resolution using calibration curve at λ_{max}.

Batch sorption experiments

Batch sorption experiments were carried out in 250 mL conical flask at 25°C under strirring conditions. Stock solutions of Calma and AB25 were prepared without pH adjustment. The concentration of acid dyes in solution was carried out from the analytical curves obtained in an ultraviolet-visible spectrophotometer with λ_{max} = 526 nm for Calma and 600 nm for AB25. About 300 mg of wet [Cu(II)/Glut-chitosan] microspheres and 100 mL of the standard solutions were stirred for a certain period. For pH effect studies, the adsorption of Calma and AB25 was tested in pH range 3–10, through adjusting pH using either HCl or NaOH (0.10*M*). While the pH sorption of Cu(II) ions ranged from 3 to 7. Equation (2) was used to calculate the amount of adsorption of either Cu(II) ions, AB25 or Calma at equilibrium:

$$q_e = \frac{(C_0 - C_e) \cdot V}{m} \quad (2)$$

where q_e is the sorption capacity of the adsorbent (mg g^{-1}), C_0 is the initial concentration of the adsorbate (mg L^{-1}), C_e is the residual concentration of the adsorbate (mg L^{-1}), when sorption is completed, that is, infinity sorption [$C_\infty = C_e$], m is the weight of the adsorbent (g), and V is the volume of the dye solution used for sorption (L).

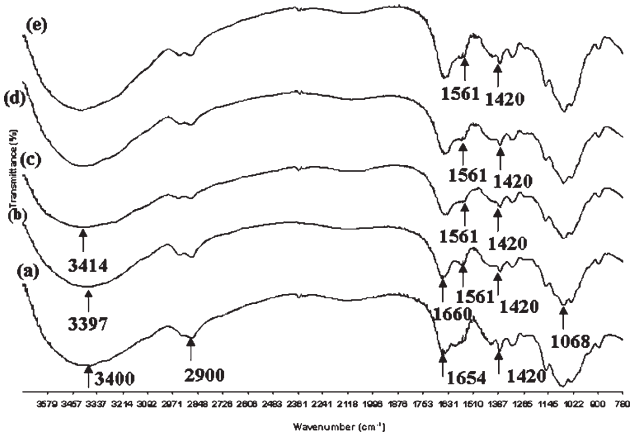

Figure 2 FTIR transmission spectrum of (a) chitosan, (b) Glut-chitosan, (c) [Cu(II)/Glut-chitosan], (d) [AB25/Cu(II)/Glut-chitosan], and (e) [Calma/Cu(II)/Glut-chitosan].

RESULTS AND DISCUSSION

Formation mechanism of the chitosan microspheres

The method of coacervation/precipitation is based on the physicochemical property of chitosan since it is insoluble in alkaline pH medium, but precipitates/coacervates when it comes in contact with alkaline solution. In the process of precipitation and crosslinking as described above, chitosan microspheres were solidified by formation of Schiff's base with the bi-functional crosslinker. The Schiff's bases formed between an amine and an aldehyde are intensely colored (yellow color). Upon introducing wet chitosan microspheres into glutaraldehyde solution, the aldehyde groups react immediately with the $-NH_2$ groups along the chitosan chains. The reaction of chitosan microspheres with glutaraldehyde in an aqueous solution might be crosslinked at amino groups to form the glutaraldehyde crosslinked chitosan. According to Yu and Tang,[40] there is also an alternate route of crosslinking besides the Schiff's base: addition to the ethylenic bond, the aldehyde-alcohol condensation reaction between glutaraldehyde molecules will lead to the formation of α,β-unsaturated oligomers.

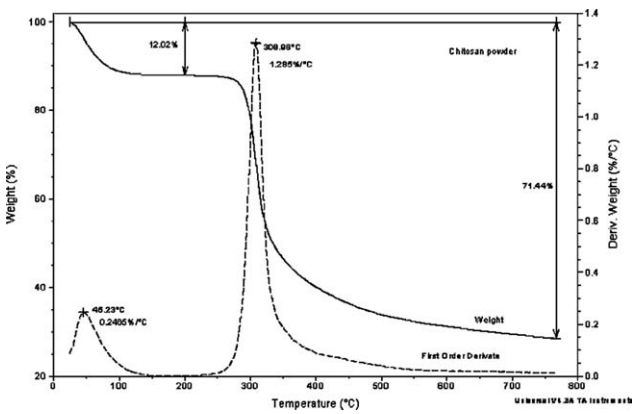

Figure 3 TG curves obtained under nitrogen atmosphere flowing at a rate of 25 mL min^{-1} and at a heating rate of 10°C min^{-1} of chitosan polymer.

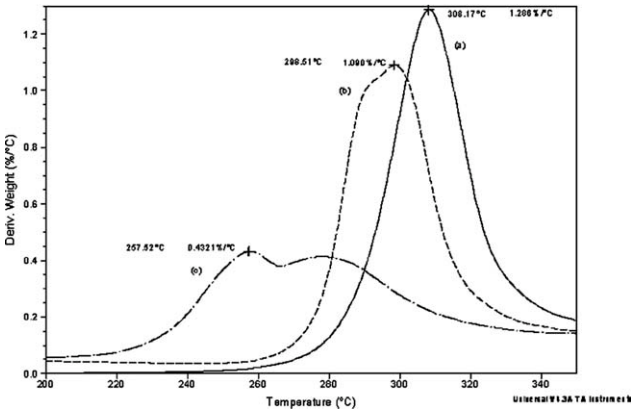

Figure 4 DTG curves obtained under nitrogen atmosphere flowing at a rate of 25 mL min^{-1} and at a 10°C min^{-1} of: (a) raw chitosan, (b) chitosan microspheres, and (c) Glut-chitosan.

FTIR spectroscopy analysis

The infrared spectrum of the raw chitosan polymer is given in Figure 2(a). Results revealed an absorption band at 3400 cm^{-1}, relatively intense because of OH and water stretching vibrations, whereas the band at 2900 cm^{-1} corresponds to the C—H stretching vibrations. The bands at 1654 and 1420 cm^{-1} may be attributed to the deformation vibrations of medium intensity of *N*—H bonds from primary amines and of low intensity from C—H bonds of the CH_3 group. The band at 1068 cm^{-1} corresponds to the stretching vibrations of C—O bonds from primary alcohol.[8,41] It is possible, from Figure 2(b,c) showing the FTIR spectrum of Glut-chitosan microspheres and [Cu(II)/Glut-chitosan] system, respectively, to explain the chemical modifications of the chitosan microspheres. In fact, in the Figure 2(b), there was a significant new band around 1660 cm^{-1}, which can be attributed to the imine bond (C=N). Another new band at 1561 cm^{-1} was observed, and can be attributed to the ethylenic bond (C=C) as already explained by Ngah and Fatinathan.[42] Moreover, the reduction of the band intensity at 1420 cm^{-1} (primary amino group,$-NH_2$) showed that most of the primary amino groups of chitosan were involved in the crosslinking process, denoting that these groups were bound to the glutaraldehyde molecules. The most obvious difference in the spectra for Glut-chitosan [Fig. 2(b)] and [Cu(II)/Glut-chitosan] [Fig. 2(c)] was observed to be the shift of the broad band for OH groups from 3397 to 3414 cm^{-1}, indicating that an amount of hydroxyl groups also interact with the Cu(II) ions.

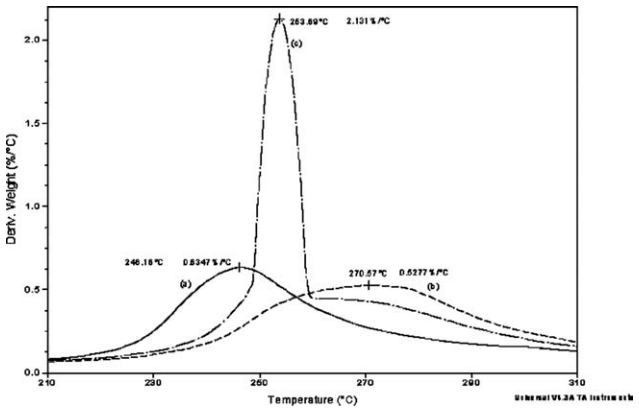

Figure 5 DTG curves obtained under nitrogen atmosphere flowing at a rate of 25 mL min^{-1} and at a rate of 10°C min^{-1} of: (a) [Cu(II)/Glut-chitosan], (b) [AB25/Cu(II)/Glut-chitosan], and (c) [Calma/Cu(II)/Glut-chitosan].

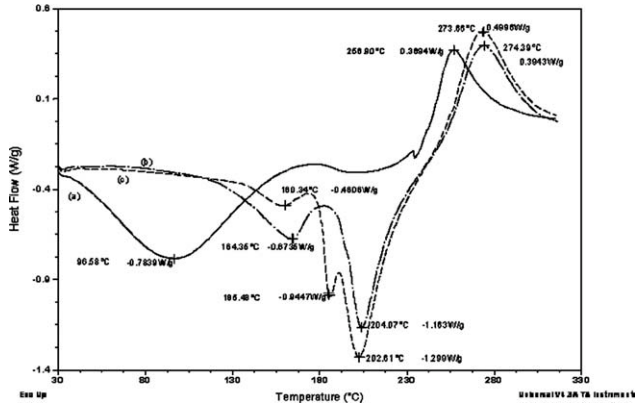

Figure 7 DSC curves obtained under nitrogen atmosphere flowing at a rate of 25 mL min^{-1} and at a heating rate of 10°C min^{-1} of: (a) [Cu(II)/Glut-chitosan], (b) [AB25/Cu (II)/Glut-chitosan], and (c) [Calma/Cu(II)/Glut-chitosan].

Transmission FTIR spectrum, measured for the binary [Cu(II)/Glut-chitosan] system before and after adsorption of Calma and AB25 as ligands, were given in Figure 2(d,e). No significant change in the band intensity was observed after dyes adsorption. This implies that the adsorption processes are physical adsorption and may not involve a chemical interaction.[26] The similar observations were also reported by Xue et al.,[43] Wan Ngah et al.,[44] and Dolphen, et al.,[45] when the adsorption of acid dyes onto modified chitosan was evaluated.

Thermal analysis

Thermogravimetry analysis (TG)

The typical TG thermogram of the raw chitosan polymer is given in Figure 3. We observed two stages of mass loss. This should be visualized as resulting from the thermal degradation of short and long molecular chains of chitosan.[46] Figure 4(a–c) showed the DTG curves of native chitosan [Fig. 4(a)], chitosan microspheres [Fig. 4(b)], and Glut-chitosan [Fig. 4(c)], respectively. The decomposition temperature observed at 308°C can be attributed to the maximum mass loss of the native chitosan. Figure 4(b) revealed that the chitosan microspheres decomposed at 298°C. While the crosslinking ones decomposed at 257°C [Fig. 4(c)]. It is also possible, from Figure 8(a–c) to assess the weight loss behavior of chitosan microspheres after Cu(II) ions and dye adsorption. Data indicated that the binary [Cu(II)/Glut-chitosan] system decomposed at 246°C [Fig. 5(a)], whereas the ternary [AB25/Cu(II)/Glut-chitosan] [Fig. 5(b)] and [Calma/Cu(II)/Glut-chitosan] [Fig. 5(c)] complexes decomposed at 270 and 253°C, respectively. Comparing all decomposition temperatures, we observed that the modification of the polymer decreased the thermal stability of the microspheres with respect to that of the native chitosan polymer.

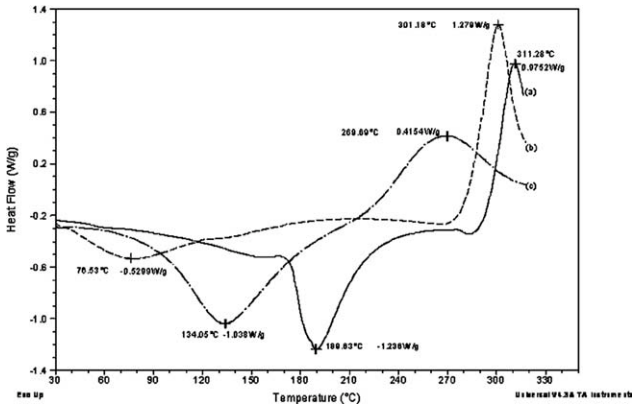

Figure 6 DSC curves obtained under nitrogen atmosphere flowing at a rate of 25 mL min^{-1} and at a heating rate of 10°C min^{-1} of: (a) raw chitosan, (b) chitosan microspheres, and (c) Glut-chitosan.

Differential scanning calorimetry analysis (DSC)

The typical DSC thermograms of native chitosan, chitosan microspheres, and Glut-chitosan were shown in Figures 6(a–c). The endothermic peak at around 76–189°C, corresponding to the water removal in the polysaccharide, can be observed for all samples. Such event confirmed the results obtained by TG. The thermogram [Fig. 6(a)] for raw chitosan showed a broad endothermic peak at 189°C and a sharp exothermic peak at 311°C, which is related to the thermal decomposition of the material. For chitosan microspheres [Fig. 6(b)], the exothermic peak is observed at 301°C. The position of this peak was shifted to lower temperatures; 269, 257, 273, and 274°C for Glut-chitosan [Fig. 6(c)], [Cu(II)/Glut-chitosan] [Fig. 7(a)], [AB 25/

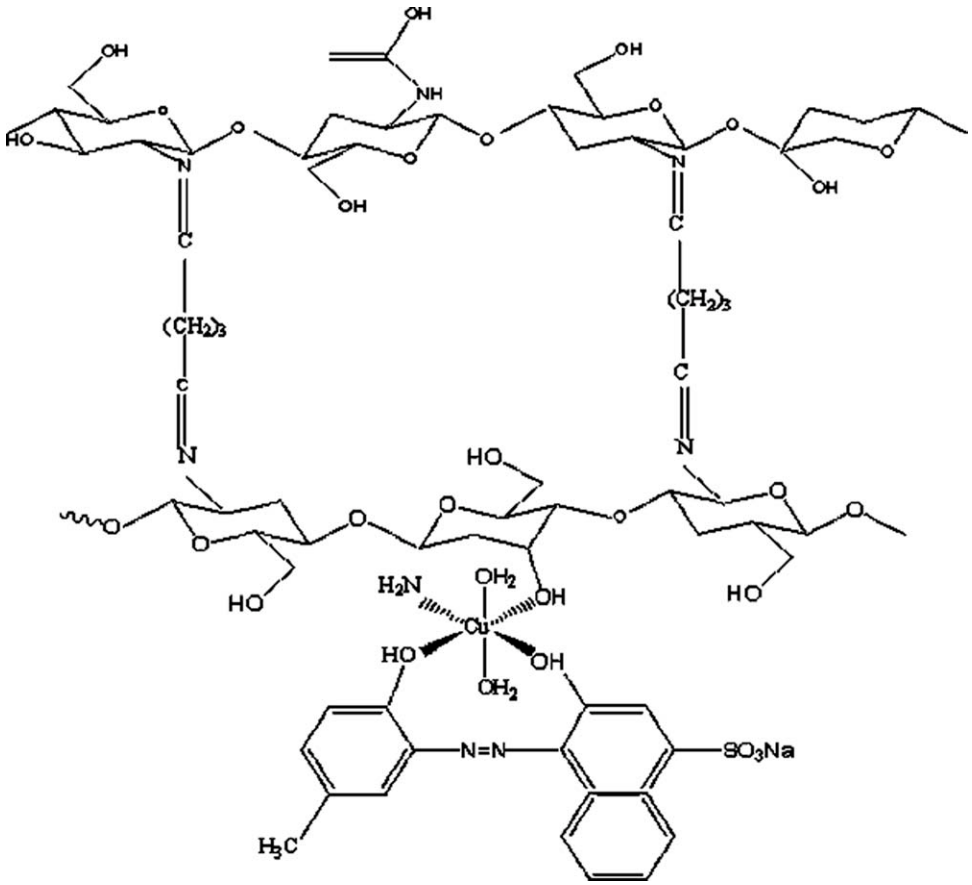

Figure 8 Proposal of associative structures between binary [Cu(II)/Glut-chitosan] system and Calma.

Cu(II)/Glut-chitosan] [Fig. 7(b)] and [Calma/Cu(II)/Glut-chitosan] [Fig. 7(c)], respectively.

The results gleaned from TG, DTG, and DSC analyses, during this study, showed a structural difference between the native chitosan, the chitosan microspheres, the binary [Cu(II)/Glut-chitosan] system, and the formed ternary [dye molecules/Cu(II)/Glut-chitosan] complex. FTIR transmission analyses and thermal studies allow us to attribute the structure indicated in Figure 8 to the possible complex. The chitosan can coordinate with Cu(II) ions through both oxygen and nitrogen atoms present in the chitosan chain. Also, when applied to the sorption bath, the two ligands including donors' atoms in their structure (Nitrogen or/and Oxygen) could bind [Cu(II)/Glut-chitosan] throughout the *d* vacant orbital of the transition metal.

Surface morphology of the prepared solid supports

Initial results obtained from optical microscopy analysis showed that the obtained particles revealed a spherical geometry. A better understanding of the morphological characteristics is then provided by SEM studies. Typical SEM micrographs of the prepared microspheres are given in Figures 9 and 10. Figure 9 showed the whole image of chitosan microspheres and Figure 10 the details of the surface structure of chitosan, Glut-chitosan, [Cu(II)/Glut-chitosan], and [Calma/Cu (II)/Glut-chitosan], respectively. The main characteristic is the porous internal structure for Glut-chitosan microspheres. The chitosan microspheres displayed a rough and a nonporous surface [Fig. 10(a)]. While the Glut-chitosan microspheres displayed a rough and macroporous structure that may be due to the agent cross-linked to chitosan. In this case, the diameters of the pores range from 50 to 158 nm [Fig. 10(b)]. The porous structure of prepared Glut-microspheres may offer more adsorption sites for adsorbate. According to the International Union of Pure and Applied Chemistry (IUPAC) classifications, the pores can be divided into macropores ($d > 50$ nm), mesopores ($2 < d < 50$ nm), and micropores ($d < 2$ nm). In this work, Glut-chitosan microspheres (d – 116 nm) can be seen as macropores compounds.

Factors affecting dye sorption on the surface of [Cu(II)/Glut-chitosan]

Effect of the pH on the adsorption of Cu(II) and dyes

In this section, the effect of the pH on the adsorption of Cu(II) ions and dye molecules on the Glut-chitosan

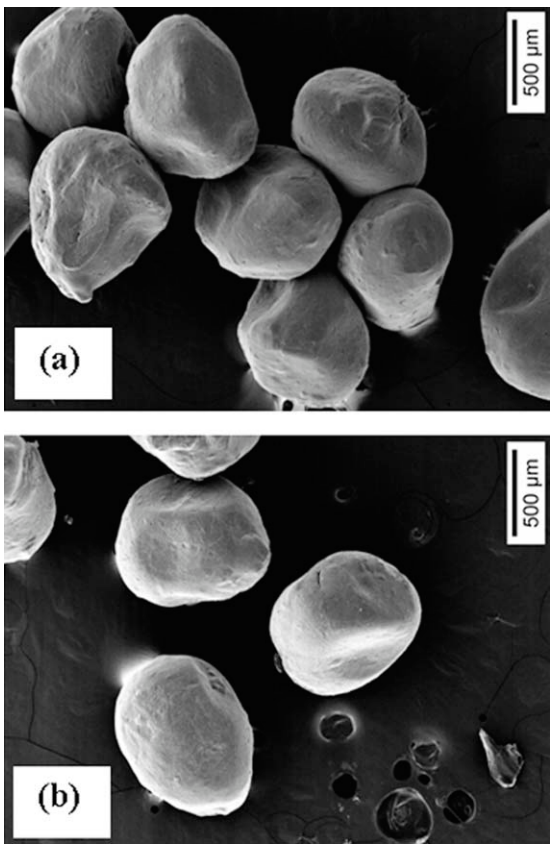

Figure 9 SEM images of whole and external surface of (a) Glut-chitosan and (b) [Cu(II)/Glut-chitosan].

microspheres was studied and depicted in Figure 11. For the adsorption of Cu(II), it was observed that the increase of the pH of the aqueous Cu(II) ions solution from 3 to 6 caused a significant increase in the amount of the adsorption capacity and reached a maximum value at pH 6. At low pH (<3), the adsorption decreases, and it can be explained by the possible protonations of the amine groups shielded by the Glut-chitosan microspheres. This protonation prevents their approach to the polymer surface. The same results were previously observed for the adsorption of Cu(II) ions on the surface of ED-cotton.[7] The removal of AB25 and Calma by Glut-chitosan as a function of pH demonstrated a different trend [Fig. 11]. The high adsorption yield was obtained at pH 5 and 4 for AB25 and Calma, respectively. The explanation of this result is that, at very low pH, protonation of anionic sulfonate groups of studied dyes prevents their adsorption on the surface of the adsorbent. In addition most of the amine groups ($-NH_2$) will be also protonated, which hinder the electrostatic interactions between acid dyes and adsorbent. The similar trend was also mentioned by Chiou et al., [47] At pH >7, the adsorption of both dyes decreased dramatically. This could be explained by the fact that at high pH, more OH^- will be available in the aqueous solution and protonation of amine groups of the adsorbent will not occur.[7]

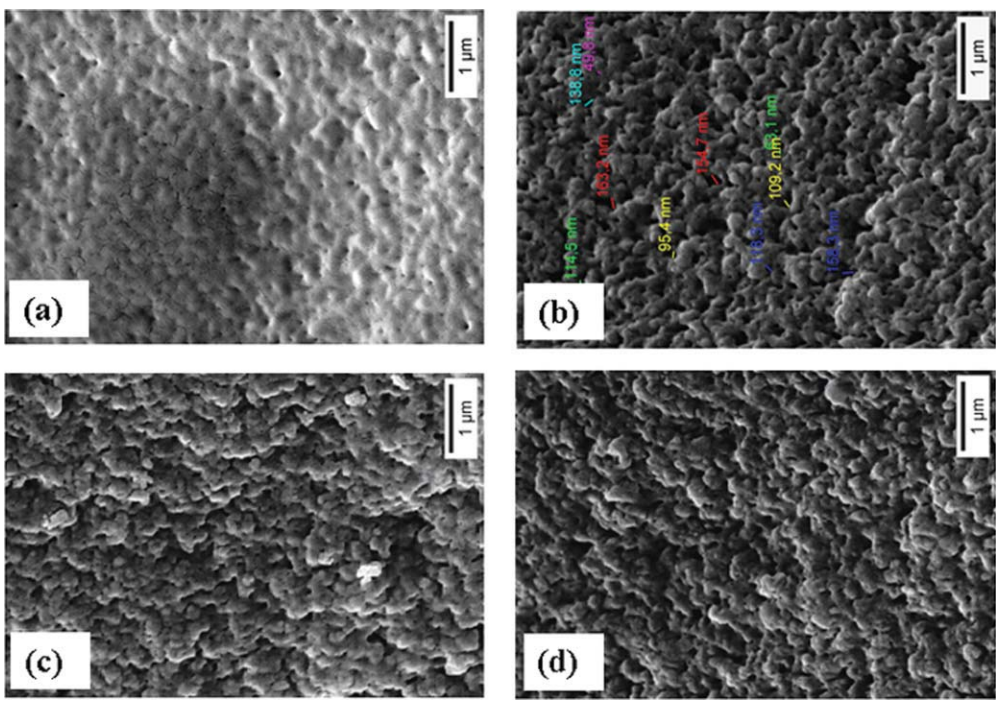

Figure 10 SEM images (details of the surface structure) of (a) chitosan, (b) Glut-chitosan, (c) [Cu(II)/Glut-chitosan], and (d) [Calma/Cu(II)/Glut-chitosan] microspheres. [Color figure can be viewed in the online issue, which is available at wileyonlinelibrary.com.]

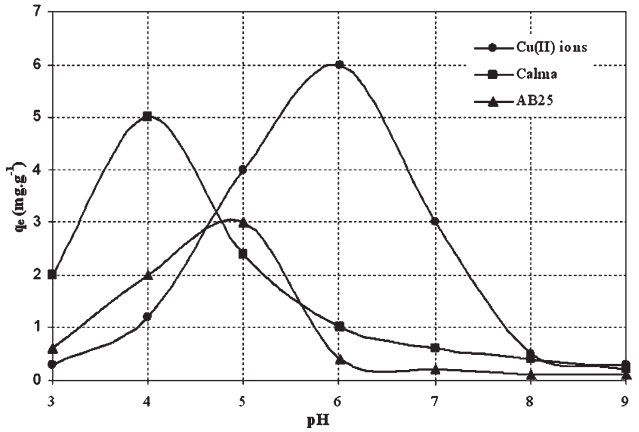

Figure 11 Effect of the initial pH on the adsorption of Cu(II) ions, Calma and AB25 (C_e = 100 mg L^{-1}) on the surface of Glut-chitosan microspheres.

Effect of the agitation period

Figure 12 shows the time required to reach equilibrium for the adsorption process. As it can be seen, fast rates of equilibration, about 50%, of dye-ion removal was achieved after 70 min and reached a steady state after 110 to 140 min for Calma and AB25. Results also indicated that the adsorption of both dyes increased with agitation period and attained equilibrium at 120 min for calma and 130 min for AB25, respectively. In addition, the kinetics was characterized by a fast initial rate followed by stabilization at high time values. Results for Calma revealed that [Cu(II)/Glut-chitosan] microspheres have higher dye removal capacities than AB25. Such event could probably be attributed to the structure and affinity effects of dyes toward adsorbent. Other several parameters, including initial dye concentration and structural properties of the adsorbent (size, surface area, and porosity) can also affect the sorption rate for both dyes.

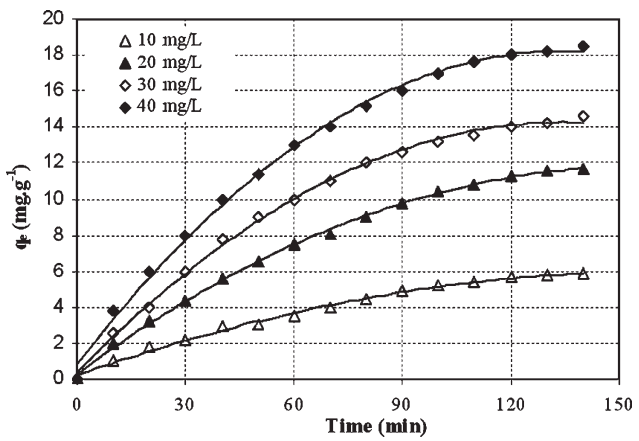

Figure 12 Effect of agitation period on the adsorption of Calma on [Cu(II)/Glut-chitosan].

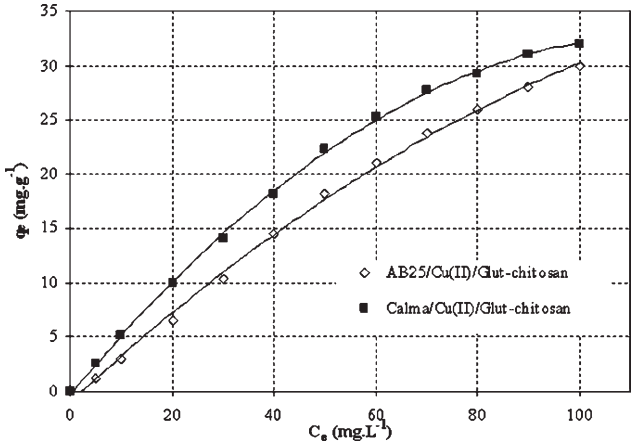

Figure 13 Effect of initial concentration on the adsorption of dyes on [Cu(II)/Glut-chitosan].

Effect of the initial dye concentration

The effect of the initial concentration on the adsorption of Calma on the surface of binary [Cu(II)/Glut-chitosan] system was studied in a wide range of concentration and given in Figure 13. All the experiments were realized at pH 6, where the highest adsorption of Cu(II) ions on the surface of the Glu-chitosan was observed. Data provide an increase, in dye removal capacity, for [Cu(II)/Glut-chitosan] microspheres as compared to unloaded ones [Fig. 11]. Maximum dyes adsorption on the [Cu(II)/Glut-chitosan] were 32 mg g^{-1} and 30 mg g^{-1} for Calma and AB25, respectively. Under the similar pH conditions and when the unloaded Glut-chitosan microspheres was used as adsorbent, adsorption capacities do not exceed 5 mg g^{-1} for Calma and 3 mg g^{-1} for AB25. These results indicate that the dyes can act as efficient ligands for coordinating metals already involved in Glut-chitosan complex.[7] Indeed at pH 6, the absence of metal ions in the filtrate confirms the

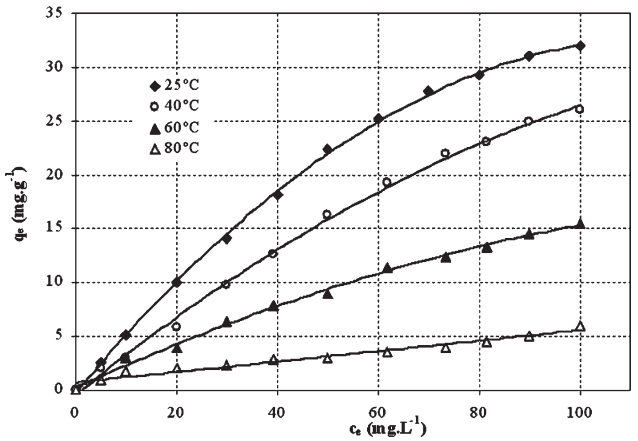

Figure 14 Effect of temperature on the adsorption of Calma on [Cu(II)/Glut-chitosan].

TABLE I
Summary of Kinetic Equations Used for the Modeling of Dye Sorption on [Cu(II)/Glut-Chitosan] Microspheres

Model	Equation	Modeling
First Order	$\frac{dq_t}{dt} = k_1(q_e - q_t)$	$\log (q_e - q_t) = \log q_e - K_1 t$
Second Order	$\frac{dq_t}{dt} = k_2(q_e - q_t)^2$	$\frac{t}{q_t} = \frac{1}{K_2 q_e^2} + \frac{t}{q_e}$
Elovich equation	$\frac{dq_t}{dt} = \alpha e^{-\beta q_t}$	$q_t = \frac{1}{\beta}\mathrm{Ln}(\alpha\beta) + \frac{1}{\beta}\mathrm{Ln}t$
Intraparticle diffusion	$q_t = k_i.t^{1/2}$	$q_t = k_i.t^{1/2}$

strong complexation power of dyes toward binary system.

Effect of the temperature

The adsorption phenomenon is usually affected by many parameters, particularly the temperature. In fact, the temperature affects two major aspects of the adsorption: the equilibrium position in relation with the exothermicity or endothermicity of the process and the swelling capacity of the adsorbent. Thus, adjustment of temperature may be required in the adsorption process. The effect of the temperature on the adsorption of Calma on the surface of [Cu(II)/Glut-chitosan] is shown in Figure 14. As observed for the selected dyes, the adsorption capacity of the binary system decreases with increasing temperature. This could be explained by the enhanced magnitude of the reverse (desorption) step in the mechanism. The interactions established between [Cu(II)/Glut-chitosan] and dyes are therefore reversible in this case. This is possibly due to the exothermic effect of the surroundings during the adsorption process.[48] As observed, at 80°C, the adsorbed quantities for binary system attained 7.4 mg g^{-1} for AB25 and 6 mg g^{-1} for Calma, respectively. The lower adsoption capacities indicate also that [Cu(II)/Glut-chitosan] is no efficient as adsorbent at high temperature.

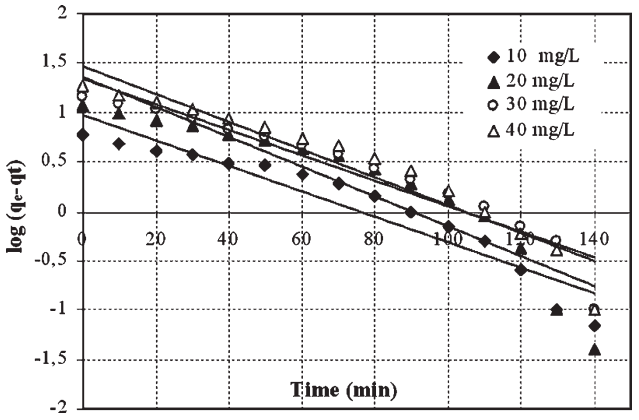

Figure 15 Pseudo first-order kinetic plots for the adsorption of Calma on [Cu(II)/Glut-chitosan].

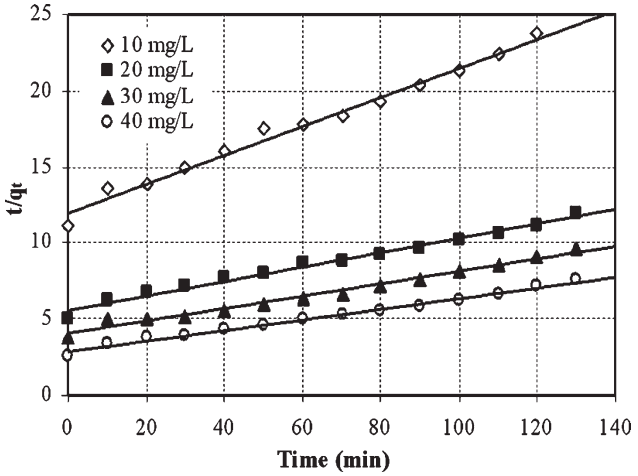

Figure 16 Pseudo second-order kinetic plots for the adsorption of Calma on [Cu(II)/Glut-chitosan].

Kinetic modeling of the adsorption of dyes on the [Cu(II)/Glut-chitosan] microspheres

To investigate the mechanism of the adsorption, the pseudo first-order,[49] the pseudo second-order,[50] the elovich,[51] and the intraparticle diffusion,[52] models were used to fit experimental data. The corresponding equations in their linear forms are summarized in Table I and the validity of each model is checked. The plots of $\log(q_e - q)$ versus time were used to determine the first-order rate constant K_1 [Fig. 15]. The plots of t/q versus time were used to calculate the second-order rate constant K_2 [Fig. 16]. The plot

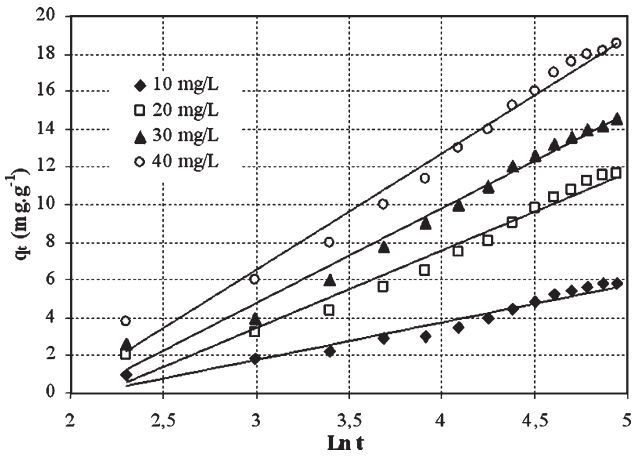

Figure 17 Elovich plots for the adsorption of Calma on [Cu(II)/Glut-chitosan].

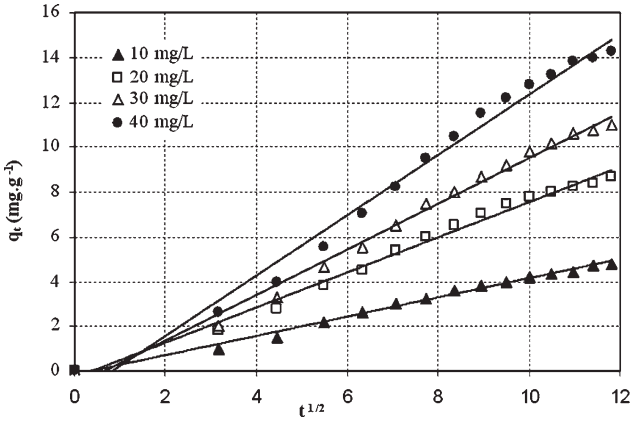

Figure 18 Intraparticle diffusion plots for the adsorption of Calma on [Cu(II)/Glut-chitosan].

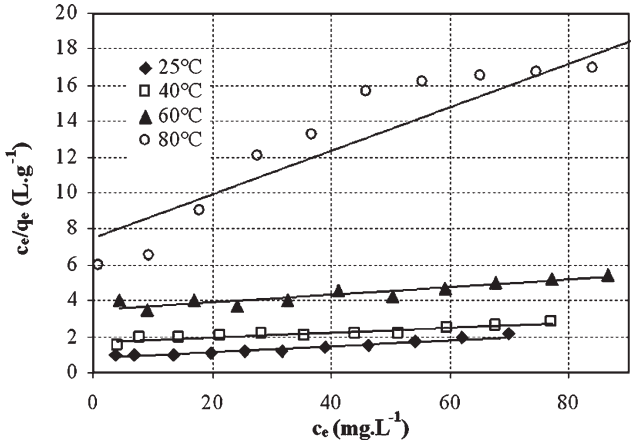

Figure 19 Langmuir plots for the adsorption of Calma on [Cu(II)/Glut-chitosan].

of q versus Ln t yielded the elovich constants, α [initial sorption rate (mg g^{-1} min^{-1})] and β [extent of surface coverage (mg g^{-1} min^{-1})] [Fig. 17]. While the plots of q versus $t^{1/2}$ yielded the intraparticle diffusion constant, K_i (mg g^{-1} min$^{1/2}$) [Fig. 18]. The results of rate constant studies for different initial dye concentration (10, 20, 30, and 40 mg L^{-1}) were tabulated in Table II. The assessment of the kinetic models is controlled by the extent of the regression coefficient R^2. In this study, the first order equation of Lagergen fits poorly to the whole range of contact time and is generally applicable over the initial stage of the adsorption processes of the studied dyes.[49] Based on the regression coefficient ($R^2 > 0.98$; Table II), the second order was shown to fit well the dye sorption. The intraparticle diffusion model was also used to describe the way of the retention of dyes on the [Cu(II)/Glut-chitosan]. If the adsorption mechanism follows the intraparticle diffusion, the plot of q versus $t^{1/2}$ should be a straight line passing through the origin.[52] The deviation of the straight line from the origin may be due to the difference between the rate of mass transfer in the initial and final stages of adsorption [Fig. 18].[53]

Analysis of the adsorption of dyes on the surface of [Cu(II)/Glut-chitosan] microspheres through Langmuir and Freundlich models

At equilibrium, there is a limited distribution of the solute between the liquid and the solid phases, which can be described by many isotherms and the adsorption models can be used to fit the observed experimental data and determine the corresponding parameters. To fit our experimental data, we have used the Langmuir[54] and Freundlich models.[55] The Langmuir equation in its linear form can be given as:

$$\frac{c_e}{q_e} = \frac{1}{Q \cdot b} + \frac{c_e}{Q} \tag{3}$$

where Q represents the adsorbate concentration in the solid phase for complete monolayer coverage or, if not possible, for the limit adsorption capacity (mg g^{-1}) on sites and b is the Langmuir constant related to the adsorption energy (L mol^{-1}). The product $Q \times b = K_L$ is the Langmuir equilibrium constant. A plot of c_e/q_e versus c_e yields the Langmuir constants

TABLE II
Kinetic Constants for the Adsorption of Studied Dyes on [Cu(II)/Glut-Chitosan] Microspheres

	First Order model			Second Order Model				Elovich Model			Intraparticle diffusion	
[Dye] (mg L^{-1})	K_1 (min^{-1})	q_e (mg g^{-1})	R^2	K_2 (g mg^{-1} min^{-1})	q_e (mg g^{-1})	h (mg g^{-1} min^{-1})	R^2	α (mg g^{-1} min^{-1})	β (mg g^{-1} min^{-1})	R^2	K_i (mg g^{-1} min$^{1/2}$)	R^2
AB25												
10	0.010	5.956	0.928	0.00184	7.007	0.090	0.993	9.969	0.657	0.984	0.427	0.991
20	0.0122	12.626	0.891	0.00095	13.037	0.162	0.994	19.213	0.354	0.981	0.788	0.989
30	0.0127	16.768	0.915	0.00057	18.018	0.187	0.995	28.622	0.268	0.978	1.022	0.989
40	0.0130	22.840	0.907	0.00037	24.752	0.231	0.983	40.526	0.201	0.970	1.347	0.984
Calma												
10	0.0129	9.613	0.905	0.00075	10.493	0.083	0.986	17.005	0.495	0.953	0.548	0.983
20	0.0152	23.062	0.85	0.0004	21.186	0.178	0.984	35.130	0.244	0.965	1.105	0.985
30	0.0129	21.877	0.914	0.00042	24.33	0.248	0.984	39.002	0.198	0.981	1.37	0.982
40	0.014	29.440	0.919	0.00042	28.653	0.347	0.993	43.044	0.161	0.980	1.717	0.988

TABLE III
Langmuir, Freundlich Constants, and Thermodynamic Parameters for the Adsorption of the Dyes on [Cu(II)/Glut-Chitosan]

		Langmuir constants							Freundlich constants		
Dye	T (°C)	Q_L (mg g^{-1})	K_L (L g^{-1})	b (L mg^{-1})	R^2	ΔH° (Kj mol^{-1})	ΔS° (Kj mol^{-1})	ΔG° (Kj mol^{-1})	P [mg (mg $L^{-1})^{1/n}$ g^{-1}]	$1/n$	R^2
AB25	25	121.951	0.607	0.005	0.74	−25.080	−87.205	1.234	2.897	0.810	0.991
	40	71.428	0.471	0.0066	0.824			1.959	3.981	0.64	0.983
	60	30.120	0.292	0.0097	0.904			3.410	3.890	0.719	0.98
	80	15.151	0.121	0.008	0.918			6.183	2.027	0.58	0.984
Calma	25	56.818	1.282	0.022	0.964	−35.381	−116.919	0.616	2.258	0.92	0.986
	40	75.757	0.590	0.0077	0.827			1.369	1.520	0.881	0.982
	60	46.948	0.286	0.0060	0.874			3.463	2.951	0.884	0.992
	80	8.176	0.134	0.0163	0.813			5.90	2.511	0.555	0.98

[Fig. 19]. The Freundlich isotherm in its linear form is given by eq. (4):

$$\log q_e = \log P + \left(\frac{1}{n}\right) \log c_e \tag{4}$$

where c_e is the equilibrium concentration of the adsorbate (mg L^{-1}), q_e is the amount of adsorbate removed per unit mass of adsorbent (mg g^{-1}), P and n are Freundlich constants. n gives an indication about the favorability of the adsorption process. P [mg(mg $L^{-1})^{1/n}$ g^{-1}] is the adsorption capacity of the used adsorbent. Table III summarizes the parameters values for the different studied adsorbate/adsorbent systems. Based on the correlation coefficients ($0.74 < R^2 < 0.96$), the Langmuir equation fits poorly to the whole range of concentration. The Freundlich equation could be more suitable to fit experimental data, the high correlation coefficients ($R^2 > 0.98$) obtained in this study strongly supports the fact that the sorption of studied dyes follows the Freundlich model [Fig. 20]. In all cases, the value of $1/n$ were found to be less than 1 indicating that the adsorption was favorable.[56]

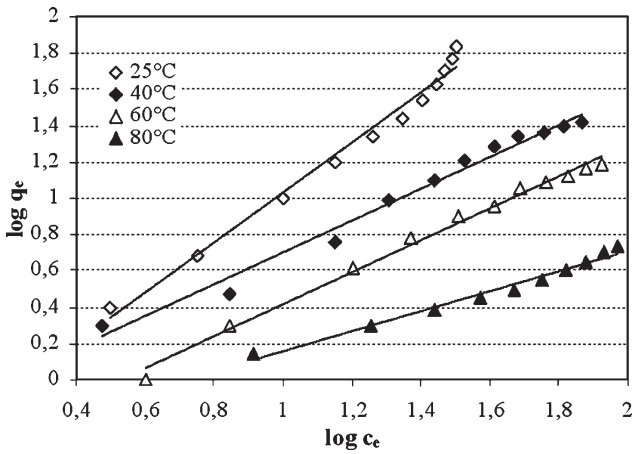

Figure 20 Freundlich plots for the adsorption of Calma on [Cu(II)/Glut-chitosan].

Thermodynamics of the sorption of dyes

The standard Gibbs free energy change (ΔG°) for the adsorption process can be calculated using the following equation[57]:

$$\Delta G^0 = -RT\mathrm{Ln}K_L \tag{5}$$

where ΔG° and T are standard Gibbs, free energy, and absolute temperature, respectively. R is the gas constant (8.314 J mol^{-1} K^{-1}) and K_L is the Langmuir equilibrium constant. lnK_L was plotted against $1/T$. The values of ΔH° and ΔS° were estimated using the following relationships[58]:

$$\mathrm{Ln}K_L = -\frac{\Delta H^0}{RT} + \frac{\Delta S^0}{R} \tag{6}$$

Figure 21 shows a plot of $\log K_L$ versus $1/T$ for the adsorption of the two tested dyes on the [Cu(II)/Glut-chitosan] microspheres. The values of ΔH° and ΔS° were so estimated and the results were reported in Table III. The associated enthalpies when the dye molecule is adsorbed on the surface of the binary system for AB25 and Calma are −25.08 and −35.38

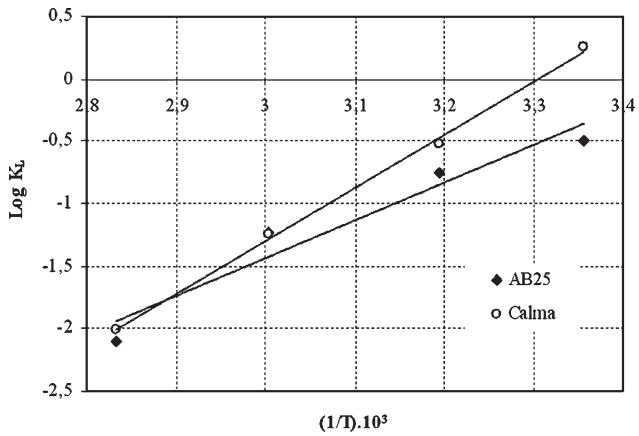

Figure 21 Log K_L versus reciprocal of temperature.

Kj mol^{-1}, respectively. The negative heat of adsorption values suggests that the interaction of the dyes with [Cu(II)/Glut-chitosan] microspheres is exothermic, which is supported by the decreasing adsorption of the corresponding dyes with the increase in temperature. In addition, heat of adsorption values indicates that the adsorption of AB25 and Calma on the support is a physical manner. This is was consistent with data discussed earlier in FTIR analyses. The negative value of the entropy change was found to be consistent with the decreased disorder at the solid-solution interface during the adsorption process. It is also possible to observe an increase in the values of $T \times \Delta S^\circ$ with increasing temperature and $|\Delta H^\circ| < |T \times \Delta S^\circ|$. This indicates that the sorption process is dominated by entropic rather than enthalpic changes.[59]

CONCLUSIONS

To sum up, [dye molecules/copper(II)/macroporous Glut-chitosan] microspheres complex was prepared using a simple way. Some characteristics of the chitosan microspheres formation via a coacervation/precipitation method were studied. The detailed information of the microspheres surface was investigated using FTIR, TG, DTG, and DSC analyses. The morphology and the surface structure of the prepared solid supports were provided by SEM. Thermal analyses showed that the modification of the polymer decreased the thermal stability of the formed materials as compared to the plain chitosan. A probable reaction mechanism of the ternary complex formation was also proposed. Thermodynamic and kinetic experiments were detailed. The pseudo second-order equation was shown to fit adsorption kinetics. The modeling of the adsorption isotherms by Freundlich equation has been confirmed and the thermodynamic parameters were determined. These parameters allowed us to deduce some results related to the exothermic nature of the adsorption phenomenon and the evolution of the disorder during the adsorption of dyes. Both heat of adsorption values and FTIR interpretation confirmed that the adsorption of AB25 and Calma on the surface of [Cu(II)/Glut-chitosan] followed a physical mode.

Globally, we have observed that the use of the macroporous Glut-chitosan microspheres in binding either metal ions and/or ligands are worthy of exploration in the context of the synthesis of ternary complexes. This paper can provide quantitative and qualitative information on the binding characteristic of Cu(II) ions with a binary system [Cu(II)/Glut-chitosan] or both Cu(II) ions and dyes with a ternary complex [Dye/Cu(II)/Glut-chitosan]. This work can be further extended for the oxidative degradation of more toxic derivatives such as pesticides using [Cu(II)/Glut-chitosan] microspheres.

NOMENCLATURE

α	Initial sorption rate (mg g^{-1} min^{-1})
b	Langmuir constant (L mg^{-1})
β	Extent of surface coverage (mg g^{-1} min^{-1})
C_0	Initial concentration of dye solution (mg L^{-1})
C_e	Concentration of the dye at equilibrium (mg L^{-1})
C_t	Breakthrough dye concentration (mg L^{-1})
D	Diameter of the pores
DA	Deacetylation degree
DTG	Derivative thermogravimetry
DSC	Differential scanning calorimetry
ΔG°	Free energy of adsorption(Kj mol^{-1})
ΔH°	Enthalpy of adsorption (Kj mol^{-1})
ΔS°	Entropy of adsorption (Kj mol^{-1})
FTIR	Fourrier Transform Infra Red
K_1	The first-order rate constant
K_L	Langmuir equilibrium constant (L g^{-1})
K_2	The second-order rate constant
λ_{max}	Maximum wavelength
N	Adsorption intensity
P	Measure of adsorption capacity [mg(mg $L^{-1})^{1/n}$ g^{-1}]
pH	Potential hydrogen
q_e	Amount of dye adsorbed at equilibrium (mg g^{-1})
q_t	Amount of dye adsorbed at time t (mg g^{-1})
R	Universal gas constant (Kj mol^{-1} K^{-1})
SEM	Scanning electron microscopy
TGA	Thermogravimetry analysis
V	Volume of the dye solution used for sorption (L)
W_{wet}	Weight of the wet microspheres
W_{dry}	Weight of the dry microspheres

References

1. Stephenson, R. J.; Sheldon, J. B. Water Res 1996, 30, 781.
2. Salem, I. A.; El-maazawi, M. Chemosphere 2000, 41, 1173.
3. Chiou, M. S.; Chuang, G. S. Chemosphere 2006, 62, 731.
4. Poots, V. J. P.; Mckay, G.; Healy, J. J. Water Res Kidlington 2003, 10, 1061.
5. Mckay, G.; Alexander, F. Chem Eng 1977, 319, 243.
6. Baouab, M. H. V.; Gauthier, R.; Gauthier, H.; Chabert, B.; Rammah, M. B. J Appl Polym Sci 2000, 77, 171.
7. Baouab, M. H. V.; Khalfaoui, M.; Gauthier, R. J Appl Polym Sci 2007, 103, 1389.
8. Muzzarelli, R. A. A. 'Chitin'. Pergamon Press: Oxoford, 1978.
9. Mckay, G.; Blair, H. S.; Gardner, J R. J Appl Polym Sci 1982, 27, 3043.
10. Cha, Y. K.; Choi, H. M.; Hyeon, T. C. J Appl Polym Sci 1997, 63, 725.
11. Elson, C. M.; Davies, D. H.; Hayes, E. R. Water Res 1980, 14, 1307.

12. Kawamura, Y.; Yoshida, H.; Asai, S. Sep Sci Technol 1959 1997, 32.
13. Bassi, R.; Prasher, S. O.; Simpson, B. K. Sep Sci Technol 2000, 35, 547.
14. Evans, J. R.; Davids, W. G.; MacRae, J. D.; Amirbahman, A. Water Res 2002, 36, 3219.
15. Ohga, K.; Kurauchi, Y.; Yanase, H. Bull Chem Soc Japan 1987, 60, 444.
16. Coughlin, R. W.; Deshaies, M. R.; Davis, E. M. Environ Prog 1990, 9, 35.
17. Helder, L.; Vasconcelos, E. G.; Laus, R.; Vitali, L.; Valfred, T. F. Mater Sci Eng C 2009, 29, 613.
18. Wana, M. W.; Kan, C. C.; Rogel, B. D.; Dalida, M. L. P. Carbohydr Poly 2010, 80, 891.
19. Kannamba, B.; Reddy, K. L.; Apparao, B. V. J Hazard Mater 2010, 175, 939.
20. Ngah, S. W. S.; Fatinathan, W. Chem Eng J 2008, 143, 62.
21. Zalloum, H. M.; Al-Qodah, Z.; Mubarak, M. S. J Macromol Sci Pure Appl Chem 2009, 46, 46.
22. Kawamura, Y.; Yoshida, H.; Asai, S.; Tanibe, H. Water Sci Technol 1997, 35, 97.
23. Guibal, E.; Milot, C.; Tobin, J. M. Ind Eng Chem Res 1998, 37, 1454.
24. Guibal, E.; Milot, C.; Roussy, J. Sep Sci Technol 2000, 35, 1021.
25. Guibal, E.; Jansson, C. M.; Saucedo, I.; LeCloirec, P. Langmuir 1995, 11, 591.
26. Kamari, A.; Ngha, W. S. W.; Liew, L. J Environ sci 2009, 21, 296.
27. Cestari, A. R.; Eunice, F. S.; Vieira, J. A. M. J Hazard Mater 2008, 160, 337.
28. Sun, W. Q.; Payne, G. F.; Moas, M. S. G. L.; Chu, J. H.; Wallace, K. K. Biotechnol Prog 1992, 8, 179.
29. Magalhaes, J. M. C. S.; Machado, A. A. S. C. Talanta 1998, 47, 183.
30. Zeng, X.; Ruckenstein, E. J Membr Sci 1998, 148, 195.
31. Sulakova, R.; Hrdina, R.; Graça, M. B. Dyes Pigment 2007, 73, 19.
32. Shen, C.; Song, S.; Zang, L.; Kang, X.; Wen, Y.; Liu, W.; Fu, L. J Hazard Mater 2010, 177, 560.
33. Baouab, M. H. V.; Gauthier, R.; Gauthier, H.; Rammah, M. E. B. J Appl Polym Sci 2001, 82, 31.
34. Zghida, H.; Baouab, M. H. V.; Gauthier, R. J Appl Polym Sci 2003, 87, 1660.
35. El Ghali, A.; Baouab, M. H. V.; Roudesli, M. S. J Appl Polym Sci 2010, 116, 3148.
36. Rorrer, L. G.; Hsien, T. Y.; Way, J. D. Ind Eng Chem Res Washington 1993, 32, 2170.
37. Vieira, R. S.; Beppu, M. M. Water Res 2006, 40, 1726.
38. Ngah, W. S.; Fatinathan, S. Colloids Surf A 2007, 277, 214.
39. Li, N.; Bai, R. B. Sep Purf Technol 2005, 42, 237.
40. Yu, J. T.; Tang, X. X. Southeast Technology University Press: Shanghai, 1991; p 191.
41. Domszy, J. G.; Roberts, A. F. Macromolecules 1985, 186, 1671.
42. Ngah, W. S.; Fatinathan, S. Chem Eng J 2008, 143, 62.
43. Xue, A. F.; Qian, S. H.; Huang, G. Q.; Han, X. F. Analyst 2001, 126, 239.
44. Ngah, W. S.; Kamari, A.; Fatinathan, S.; Ngah, P. W. Adsorption 2006, 12, 249.
45. Dolphen, R.; Sakkayawong, N.; Thiravetyan, P.; Nakbanpote W. J Hazard Mater 2007, 145, 250.
46. Kanaul, J. Z.; Kasaai, M. R.; Bui, V. T.; Creber, K. A. M. J Chem 1998, 76, 1699.
47. Chiou, M. S.; Li, H. Y. Chemosphere 2003, 50, 1095.
48. Rattanaphani, S.; Chairat, M.; Bremner, J.; Rattanaphani, V. Dyes Pigment 2007, 72, 88.
49. McKay, G.; Ho, Y. Water Res 1999, 33, 578.
50. McKay, G.; Ho, Y. Process Biochem 1999, 34, 451.
51. Örnek, A.; Özacar, M.; Şengil, I. A. Biochem Eng J 2007, 37, 192.
52. Grini, G.; Peindy, H. N.; Gimbert, F.; Robert, C. Sep Purif Technol 2007, 53, 97.
53. Panday, K. K.; Prasad, V. N. Environ Technol Lett 1986, 50, 547.
54. Langmuir, I. J Am Chem Soc 1918, 40, 1361.
55. Freundlich, H. Colloid and Capillary Chemistry; Mateun: London, 1926.
56. Treybal, R. E. Mass Transfer Operations; McGraw-Hill: New York, 1987.
57. Aksu, Z.; Tezer, S. Process Biochem 2000, 36, 431.
58. Gupta, V. K.; Mittal, A.; Krishnan, L.; Gajbe, V. J Sep Purif Technol 2004, 40, 87.
59. Kyzas, G. Y.; Kostoglou, M.; Lazaridis, N. K. Chem Eng J 2009, 152, 440.